Research article

Emissions from a modern log wood masonry heater and wood pellet boiler: Composition and biological impact on air-liquid interface exposed human lung cancer cells

Tamara Kanashova[1,4,7], Olli Sippula[1,5], Sebastian Oeder[1,2,3], Thorsten Streibel[1,7,8], Johannes Passig[1,8], Hendryk Czech[7], Tony Kaoma[15], Sean C. Sapcariu[1,6], Marco Dilger[1,9,10], Hanns-Rudolf Paur[1,9], Christoph Schlager[1,9], Sonja Mülhopt[1,9], Carsten Weiss[1,10], Carsten Schmidt-Weber[2], Claudia Traidl-Hoffmann[3,12], Bernhard Michalke[13], Tobias Krebs[1,14], Erwin Karg[8], Gert Jakobi[8], Sorana Scholtes[1,8], Jürgen Schnelle-Kreis[8], Martin Sklorz[7], Jürgen Orasche[8], Laarnie Müller[8], Ahmed Reda[8], Christopher Rüger[7], Anika Neumann[7], Gülcin Abbaszade[8], Christian Radischat[1,7], Karsten Hiller[1,6], Julija Grigonyte[5], Miika Kortelainen[5], Kari Kuuspalo[5], Heikki Lamberg[5], Jani Leskinen[5], Ilpo Nuutinen[5], Tiina Torvela[5], Jarkko Tissari[5], Pasi Jalava[5], Stefanie Kasurinen[5], Oskari Uski[5], Maija-Riitta Hirvonen[1,5,11], Jeroen Buters[1,2,3], Gunnar Dittmar[1,4,15], Jorma K. Jokiniemi[1,5], and Ralf Zimmermann[1,7,8]

[1] HICE – Helmholtz Virtual Institute of Complex Molecular Systems in Environmental Health – Aerosols and Health, www.hice-vi.eu
[2] Center of Allergy and Environment (ZAUM), Helmholtz Zentrum München and Technische Universität München, Munich, Germany, Member of the German Center for Lung Research (DZL)
[3] CK-CARE, Christine Kühne Center for Allergy Research and Education, Davos, Switzerland
[4] Mass Spectrometry Core Unit, Max Delbrück Center for Molecular Medicine Berlin-Buch, Germany
[5] University of Eastern Finland, Department of Environmental Science, P.O. Box 1627, FI-70211 Kuopio, Finland
[6] Luxembourg Centre for Systems Biomedicine, University of Luxembourg, L-4362 Esch-Belval, Luxembourg
[7] Joint Mass Spectrometry Centre, Chair of Analytical Chemistry, Institute of Chemistry, University Rostock, Germany
[8] Joint Mass Spectrometry Centre, CMA – Comprehensive Molecular Analytics, Helmholtz Zentrum München, Neuherberg, Germany
[9] Institute for Technical Chemistry (ITC), Karlsruhe Institute of Technology, Campus North, Karlsruhe, Germany and Vitrocell Systems GmbH
[10] Institute of Toxicology and Genetics (ITG), Karlsruhe Institute of Technology, Campus North, Karlsruhe, Germany
[11] National Institute for Health and Welfare, Department of Environmental Health, P.O. Box 95, FI-70701, Kuopio, Finland
[12] Chair and Institute of Environmental Medicine, UNIKA-T, Technische Universität München and Helmholtz Zentrum München, Germany
[13] Research Unit Analytical BioGeoChemistry, Helmholtz Zentrum München – German Research Center for Environmental Health GmbH, Neuherberg, Germany
[14] Vitrocell Systems GmbH, Waldkirch, Germany
[15] Proteome and Genome Research Laboratory, Luxembourg Institute of Health, Luxembourg

*Correspondence: ralf.zimmermann@helmholtz-muenchen.de (Ralf Zimmermann)

Abstract

The consumption of wood fuel is markedly increasing in developing and industrialized countries. Known side effects of wood smoke inhalation manifest in proinflammatory signaling, oxidative stress, DNA damage and hence increased cancer risk. In this study, the composition and acute biological impact of emissions of state-of-the-art wood combustion compliances: masonry heater (MH) and pellet boiler (PB) were investigated. Therefore A549 cells were exposed to emission aerosols in an automated air-liquid interface exposure station followed by cytotoxicity, transcriptome and proteome analyses. In parallel, aerosols were subjected to a chemical and physical characterization. Compared to PB, the MH combustion at the same dilution ratio resulted in a 3-fold higher particle mass concentration (PM2.5) and deposited dose (PB: 27 ± 2 ng/cm^2, MH; 73 ± 12 ng/cm^2). Additionally, the MH aerosol displayed a substantially larger concentration of aldehydes, polycyclic aromatic hydrocarbons (PAH) or oxidized PAH. Gene ontology analysis of transcriptome of A549 cells exposed to MH emissions revealed the activation of pro-inflammatory response and key signaling cascades MAP kinase and JAK-STAT. Furthermore, CYP1A1, an essential enzyme in PAH metabolism, was induced. PB combustion aerosol activated the proinflammatory marker IL6 and different transport processes. The proteomics data uncovered induction of DNA damage-associated proteins in response to PB and DNA double-strand break processing proteins in response to MH emissions. Taking together, the MH produces emissions with a higher particle dose and more toxic compounds while causing only mild biological responses. This finding points to a significant mitigating effect of antioxidative compounds in MH wood smoke.

Keywords

Particulate matter; Wood combustion; Log wood; Wood pellets; Masonry heater; Pellet boiler; Air-liquid interface aerosol exposure; Human lung cells; Air-Toxics; Biomarkers; Proteomics; Transcriptomics; Polycyclic aromatic hydrocarbons; Phenolic compounds; Antioxidants; CYP1A1 induction; Soot; Zinc

Submitted: November 8, 2017; Accepted: November 24, 2017

1. Introduction

Air pollution is a complex mixture of gas- and particulate-phase components comprised of inorganic and organic species. Over the past decades, several epidemiological studies showed that ambient air pollution, and especially inhalable particulate matter (PM), induce severe health effects including increased rates of morbidity and mortality in the exposed populations [1–6]. Source apportionment studies reveal that globally, about 20% of urban ambient $PM_{2.5}$ air pollution is caused by domestic fuel burning. This ranges from 12% in the USA, 22% in Northwestern and 32% in Central and Eastern Europe to about 34% in Africa [7]. Increasing evidence has accumulated that smoke from burning biomass is a serious risk factor for developing chronic obstructive pulmonary disease (COPD), a widespread airway illness and a major cause of death worldwide [8, 9]. At the cellular level, several *in vitro* studies have shown the proinflammatory effects of biomass smoke exposure. Contact to wood and coal combustion from PM induced an increased production of chemokines, like monocyte chemoattractant protein (MCP)-1 and IL-8 in the NSCLC A549 cell line [10, 11], while other combustion particles induced differential pro-inflammatory responses [10, 12–15]. Mechanistically, wood smoke induces the production of reactive oxygen species (ROS) impacting on the oxidative/reductive state of the cell. This affects the production of superoxide and increases the generation of free radicals [16], which induces DNA damage [10].

The current study was prompted by the increased use of wood as a renewable fuel in industrialized countries, with the emergence of wood pellets as an alternative to wood logs. However, the use of wood as a source of energy is highly country-specific. Countries with low energy wood production or fewer forest areas (e.g. the United Kingdom) nowadays import wood pellets. In 2014, the worldwide pellet production was around 27 million tons [17]. Besides easy storage and transport, pellets are currently found to be an efficient and relatively clean fuel for residential heating. Several studies found significantly lower emissions of PM and hazardous organic substances for small-scale pellet combustion compared to log wood combustion [15, 18–21].

Toxicological studies on combustion particles exposure were mostly performed using cell systems, animals and in rarer cases human volunteers [22]. For cell culture based-research, the submersed method is commonly used for exposure experiments, where particles suspended in culture medium are applied to cells. This method is not suitable for the study of airborne particles and can result in low sensitivity for evaluating biological effects [23]. A new direction for studying direct exposures to emission aerosols has emerged with the appearance of air-liquid-interface (ALI) systems [24–26]. The ALI technology enables reproducible and direct on-site exposure of lung cell cultures to aerosols under realistic dilution, flow and humidity conditions [27] and can readily be combined with multi-omics analysis techniques [28, 29].

In this study, the composition and biological effects of combustion aerosol emissions from a log wood operated masonry heater (MH) and a modern pellet boiler (PB) are compared and discussed in the context of previously obtained results on particulate emissions from a ship diesel engine. The analysis of the biological multi-omics data combined with the physicochemical aerosol analysis provides a comprehensive overview of affected biological mechanisms and pathways, which enable to further identify potentially harmful components of the wood combustion aerosols.

2. Materials and methods

2.1. Combustion experiments

The combustion experiments were carried out at the ILMARI research facility of the University of Eastern Finland in Kuopio (*www.uef.fi/ ilmari*). Combustion of beech logs was carried out in a modern soapstone MH equipped with combustion air staging system (model HIISI, Tulikivi Ltd, Finland). This type of MH represents the current state-of-the-art of heat retaining MHs utilized in northern Europe. Wood logs are combusted in a relatively short period of time and at high power, leading to high combustion rates and firebox temperatures. The staging of the combustion air considerably decreases carbon monoxide and organic emissions in MHs when compared to conventional MHs without air staging [30]. Combustion experiments were designed for 4 h cell exposure and started in a cold (room temperature) stove. Each experiment included combustion of six batches of wood logs, taking 35 minutes each and a residual char burning phase of 30 minutes corresponding to fuel power of approximately 15 kW. The detailed information is given in the supplement (Text S1).

The PB combustion experiments were carried out using a modern automatic 25 kW PB (model PZ-RL, Biotech Energietechnik GmbH, Austria; see Fig. S1). The softwood pellets contained pine and spruce wood. The boiler was operated with factory settings and nominal load of 25 kW, which leads to particle emissions mainly consisting of alkali metal salts [31]. In all combustion experiments, the boiler was pre-heated by operating it for one hour before starting the 4 h measurements. The PB was operated under constant load conditions (typical for single-house boilers equipped with large water reservoirs) and had a very constant and stable combustion behavior. The detailed information about the sampling methods is summarized in the supplement (Text S1).

2.2. Cell culture conditions and stable isotope labeling (SILAC)

A549, human non-small cell lung cancer cells, were purchased from the American Type Culture Collection (ATCC CCL-185; *http://www. lgcstandards-atcc.org/Products/All/CCL-185.aspx*), and cultured for 6 passages in RPMI-1640 media supplemented with 10 % dialyzed FBS (Sigma-Aldrich), 100 U/ml penicillin, 100 μg/ml streptomycin (Sigma-Aldrich), and either 48.67 μg/ml H_4-lysine (lysine0, Sigma-Aldrich) or 4, 4, 5, 5-D_4-lysine (lysine4, Sigma-Aldrich) to achieve a complete labeling of the cells [32] for SILAC analysis. In order to detect unlabeled contaminants in each sample, a reverse experiment was created by swapping the lysine0 for the lysine4 label. 24 h before the experiment ca. 500.000 cells were seeded into 24mm diameter porous membrane inserts (Corning), respectively, with 0.4 μm pore size on top of the cell culture medium.

2.3. Cell exposure at air-liquid interface

The cell exposure experiments were performed in the mobile biological laboratory of the HICE consortium (HICE-mobilab, *www.hice-vi.de*), which was brought to the experimental site in Finland. Cell exposures were performed in an automated air-liquid interface exposure station (HICE ALI system by KIT, Germany and Vitrocell Systems GmbH, Germany). It is a complete system providing all process technology required for cell exposure experiments at dynamic aerosol sources under conditions imitating those of the hu-

man lung. Important parameters for cell viability and exposure such as temperature, humidity, and airflow were electronically monitored and controlled [Mülhopt et al. 2016]. The combustion aerosol was conducted through a $PM_{2.5}$ impactor to simulate deposition in the upper respiratory tract.

To provide reproducible experimental conditions for the exposure, the ALI system was used based on a previous study [33]. The aerosol was humidified by steam injection to 85% relative humidity and the temperature was set at 37°C. The flow rate was set to 100 ml/min. Cells on membrane inserts were placed into media compartments that were previously incubated with RPMI-1640 growth medium supplemented with 10 mM HEPES pH 7.3 (Life Technologies), 100 U/ml penicillin, 100 µg/ml streptomycin (Sigma-Aldrich), and either 48.67 µg/ml H_4-lysine (lysine0, Sigma-Aldrich) or 4, 4, 5, 5-D_4-lysine (lysine4, Sigma-Aldrich). Cells were exposed for 4 h with a 1:40 with compressed AADCO cleaned ambient air diluted wood combustion aerosols (Fig. 1). The experiments were performed in triplicates as 3 independent exposures.
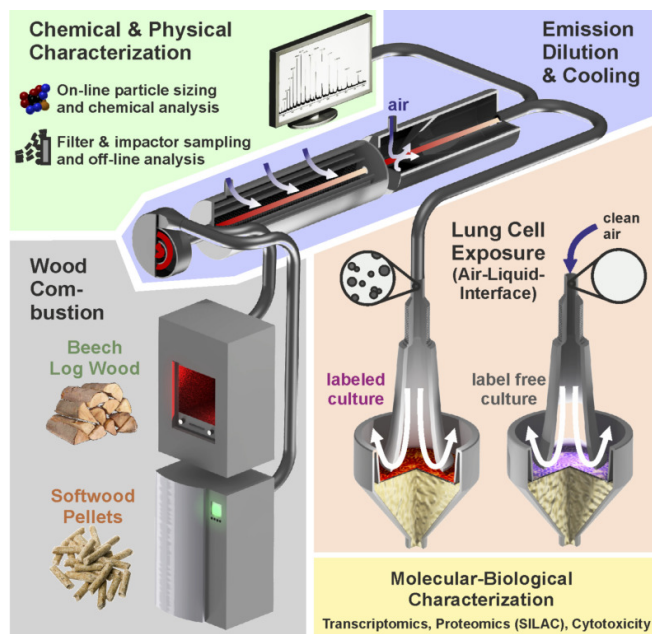

Fig. 1. Schematic representation of the experimental setup. Emission aerosols from an automatic PB or from a MH were diluted 1:40 with compressed AADCO cleaned ambient air. The combustion aerosols were physically and chemically characterized using on-line and off-line methods. A549 cells were directly exposed for 4 h at the ALI with the diluted and humidified combustion emissions with clean air as a reference and subjected to toxicological, proteomic and transcriptomic analyses.

2.4. Proteomic analysis

Protein extraction was performed directly after exposure as previously described in Sapcariu et al., [34]. 100 µg of the protein extracts (50 µg of the lysine0 and 50 µg lysine4 labeled proteins were digested using an automated sample-preparation workflow (Axel-Semrau Proteome Digest-O-r), which allowed the reproducible preparation of large numbers of samples [35]. The samples were reduced with 1 mM tris(2-carboxyethyl)phosphine (TCEP, Merck) and free sulfhydryl groups carbamidomethylated using 5.5 mM chloroacetamide (Sigma-Aldrich). Proteins were digested with

0.5 µg sequencing grade endopeptidase LysC (Wako) overnight at room temperature. The reaction was terminated by adding trifluoroacetic acid (TFA, Merck) to a final concentration of 1% resulting in a final pH of 2. The peptides were purified using C18 stage-tips (3M) [36]. The samples were measured on a Q-Exactive mass spectrometer (Thermo-Fisher, Germany) coupled to a nano-LC system (easy-nLC, Thermo-Fisher, Germany) in data-dependent acquisition mode, selecting the top 10 peaks for HCD fragmentation (Text S1). For the automatic interpretation of the recorded spectral data, the MaxQuant software package version 1.5.2.8 was employed, using a multiplicity of 2 for SILAC (unlabeled and lysine4) [37]. Carbamidomethylation was set as a fixed modification while oxidized methionine and acetylated N-termini were set as variable modifications. An FDR of 1% was applied to peptide and protein level and an Andromeda-based search was performed using a human Uniprot database (uniprot.HUMAN.2014-08.fasta, downloaded August 08th 2014). The ratios heavy/light and medium/light of the protein groups were normalized against their median using the MaxQuant. The normalized ratios of the protein Groups output file were used to determine proteins undergoing regulation.

2.5. Transcriptome analysis

Directly after aerosol exposure, cells were lysed in RLT buffer of RNeasy mini Kit (Qiagen, Germany). Total RNA was cleaned up on RNeasy mini columns (Qiagen). RNA was spiked (One-Color RNA Spike-in Kit, Agilent, Germany), reversely transcribed into cDNA with T7 primers and labeled with Cy3-coupled CTP in a T7 RNA polymerase transcription reaction (Low Input Quick Amp Labeling Kit, one-color, Agilent). Labeled cRNA was purified on RNeasy mini spin columns (Qiagen, Germany), fragmented and hybridized on microarray slides (Sure Print G3 Human Gene Expression Microarray 8 x 60 K, Agilent). After 17 h at 65°C in a hybridization oven, microarray slides were washed (Gene Expression Wash Buffer Kit, Agilent) and scanned (Agilent C microarray scanner, Agilent). Data were extracted using Feature Extraction software (Agilent).

2.6. Bioinformatics

Data obtained from the proteomics and transcriptomics analyses were log-transformed for the aerosol and clean air replicates using the R-statistical software package (version 3.3.3) [38]. Means for the six replicates (three forward and three reverse) were calculated and used for the determination of regulated proteins and means for the three biological replicates were calculated and used for the determination of regulated transcripts.

Principal component analysis was used to reduce the dimensionality of the data and to facilitate data exploration. As the third first principal components revealed a strong batch effect, ComBat [39] was applied to correct for that. The rank-product [40] was used to estimate the statistical significance of $\log_2$ ratio difference between the aerosol treated and the control group. Pfp is the adjusted p-value provided by rank-product. Genes with a pfp < 0.1 and 2.5% of the most up and downregulated and proteins with pfp < 0.1 and 25% of the most up and downregulated were selected for the further analysis (Table S1). Regulated proteins and transcripts were used for the Gene Ontology analysis using the DAVID online tool [41]. The raw data were stored in Gene Expression Omnibus (GSE93557) and Proteomics DB (PRDB004262), respectively.
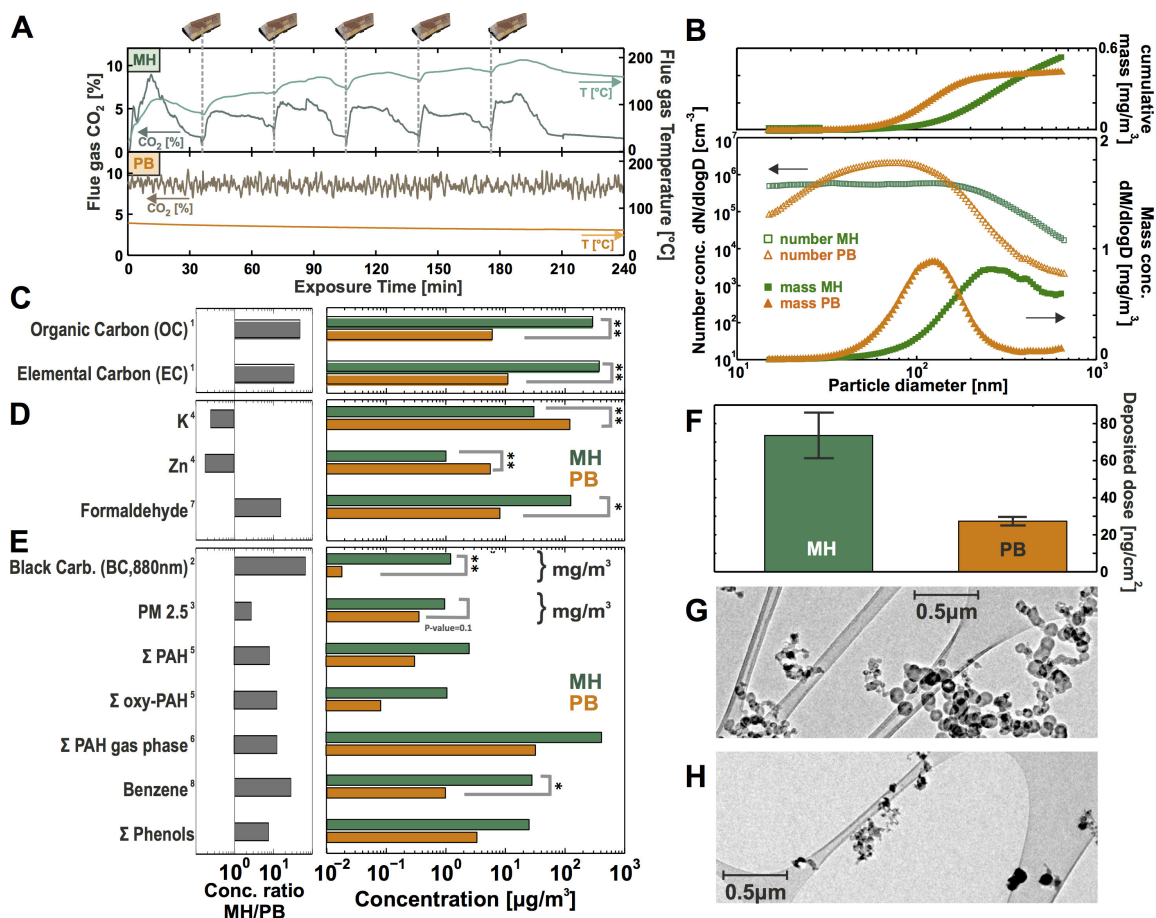
Fig. 2. Chemical and physical characterization of the wood combustion aerosols. (A) The general characterization of the combustion processes indicated by means of the temperature and CO_2 concentration of the flow gas, (B) particle number and mass distributions, (C-E) chemical aerosol analyses represented in relative concentrations (right, log scale) and absolute concentrations in bar plots (left, log scale), (F) particle deposition dose onto the cell surface in the ALI unit, (G) transmission electron microscope (TEM) images of MH and (H) PB combustion particles.

Applied methods: 1 = EC/OC-analysis (thermal-optical method), 2 = Aethalometer, 3 = Filter gravimetry, 4 = Element analysis (ICP-AES), 5 = Thermal desorption/direct derivatization gas chromatography/Mass spectrometry and comprehensive two-dimensional gas chromatography/Time-of-flight mass spectrometry, 6 = On-line photo ionization mass spectrometry (REMPI-MS), 7 = GC-SIM-MS, 8 = On-line photo ionization mass spectrometry (SPI-MS), * = p-value < 0.05, ** = p-value < 0.005.

2.7. Chemical and physical characterization of the exposure aerosol

The bulk gases of the emissions were measured continuously including carbon dioxide (CO_2), carbon monoxide (CO), oxygen (O_2) and nitrogen oxide (NOx) concentrations. Photoionization (PI) Time-of-Flight (TOF) mass spectrometry was applied to obtain a more detailed on-line analysis of the volatile organic emissions (Text S1). Furthermore, volatile carbonyl compounds (CCs) from the gas phase were analyzed, since they are known to be one of the major volatile organic compound (VOC) class released by cellulose combustion [42] and harmful to human health [43] (Text S1). The sampling of these compounds was carried out on cartridges with 2, 4-dinitrophenylhydrazine (DNPH) derivatization and subsequently analyzed by gas chromatography coupled with mass spectrometry (GC-MS).

Particle size distribution and concentration were measured by a Scanning Mobility Particle Sizer (SMPS 3080, TSI, USA). The SMPS was set to the maximum particle size range of 15 nm to 638 nm. Furthermore, particle concentrations were continuously monitored with a Condensation Particle Counter (CPC 3022, TSI, USA) [44]. Size distribution inside the ALI setup was calculated from measured number distribution data by applying the corresponding dilution factors. The mass deposited on the cell layer was estimated from $PM_{2.5}$ filter sample data assuming an overall deposition of 1.5% of the $PM_{2.5}$ exposure concentration [45–47]. $PM_{2.5}$ concentration was determined by weighing PTFE membrane filters, which were conditioned at room temperature for one hour before and after sampling.

Black Carbon (BC) which is defined as the light absorbing fraction, was measured with a 7-wavelength (370-950nm) Aethalometer (AE33, MAGEE Scientific, Slovenia), as described in Arnott et al. [48]. Since BC absorbed wavelength independently, the BC concentration was defined at 880nm. Shorter wavelength (370-450 nm) are also absorbed by organic species like substituted aromatic compounds or PAH, which represent the so-called Brown carbon (BrC) fraction. Analyses of the organic and elemental carbon (OC and EC) content were carried out by a (TOCA, Desert Research Institute

Model 2001A, USA) applying the *Improve A* protocol which defines four different fractions of (OC_I to OC_{IV}) and three fractions of elemental carbon (EC_I to EC_{III}) according to a temperature program. For the detection of several particulate organic compounds, an *in situ* derivatization thermal desorption coupled to gas-chromatography followed by a time-of-flight mass spectrometry (Leco, USA) was applied. A detailed description can be found in supplemental Text S1 and in Orasche et al. [19]. The water-soluble organic fraction was analyzed via ESI high-resolution mass spectrometry (FT-ICR MS) and elemental analysis of the particulate samples was performed by ICP atomic emission spectrometry (ICP-AES, system, Spectro Ciros Vision"system from SPECTRO Analytical Instruments GmbH & Co. KG, Kleve, Germany).

2.8. Statistical analysis

For the statistical analysis of the physical and chemical characterization of the MH and PB aerosols, the means of the replicates of three exposure experiments were calculated and shown in the plots of the absolute or relative quantification. For the determination of the statistical significance of any changes detected in the comparison between MH and PB the two samples, a two-sided t-test was applied to calculate the *p*-values. For the data visualization on a linear scale, the standard deviations are shown, and on a logarithmic scale, the *p*-values were included.

3. Results and Discussion

The general characterization of the investigated combustion processes after 4 h exposure time was depicted by means of the temperature and CO_2 concentration of the flowing gas (Fig. 2A). The MH showed a very transient and cyclic combustion behavior due to the repetitive log wood batch fillings. Each batch was characterized by an ignition phase, flaming combustion and char burning phase [49, 50]. Expectedly, in batch combustion experiments the variations are always higher than in automated combustion appliances, despite the extensive effort for high reproducibility. In contrast, the PB, which was operated under constant load conditions, had a very constant and stable combustion behavior (Fig. 2A).

3.1. Chemical and physical analyses and cell exposure dose

In the nanoparticle size region, the particle size distribution of the PB emissions reached the maximum at a lower range (~ 80 nm) in comparison to the log wood combustion emissions (~ 200 nm). The difference in peak concentration between PB and MH was more clearly visible in the derived mass size distribution (~ 105 nm and ~ 270 nm for PB and MH emissions, respectively). The particle size distribution changed very dynamically, thus the depicted information is brought as an example (Fig. 2B).

For determination of the deposited dose, the $PM_{2.5}$ concentration values from filter gravimetry were used. Assuming a size-independent, constant deposition probability of 1.5% in the applicable size range [47, 51], the accumulated particle mass deposited on the lung cell monolayer surface area was found to be 27 ± 2 ng/cm^2 for PB and 73 ± 12 ng/cm^2 for MH combustion per 4 h exposure duration. Thus, particle deposition dose is ~ 3-fold higher for the MH combustion experiments (Fig. 2F). The relatively high deposited dose for MH combustion particles was caused by larger agglomerates, which were confirmed by transmission electron microscopy (TEM; Fig. 2G).

TEM for MH particles revealed a typical fractal soot aggregate structure with a diameter of 50 nm carbon-rich primary particles (Fig. 2B and G). The PB combustion particles showed a vast predominance of small nanoparticles with the absence of larger aggregates. The particles were predominantly asymmetrically shaped and below a diameter of 200 nm (Fig. 2B and H).

Fig. 2C-E summarize the chemical composition of the MH and PB aerosol in a bar graph (selected parameters). Fig. 2C and black carbon from 2E depict the $PM_{2.5}$ concentration and the carbon fractions according to thermal-optical carbon analysis (elemental carbon (EC) and organic carbon (OC)) as well as the optically determined black carbon (BC) value. This shows that MH combustion particles contained high amounts of refractory EC and non-refractory OC. The PB emissions showed much lower concentrations for all carbonaceous fractions. The emissions of both wood combustion compliances revealed high contributions of inorganic ash species, particularly potassium and zinc. Note that potassium is a well-known tracer/biomarker for wood combustion [52, 53] and zinc is a toxic constituent of wood smoke particles [14, 54].

In the supplementary Fig. S5A the results of the elemental analysis of the PM are summarized. Most of the ash species (sulfur, sodium, potassium, and zinc) were higher concentrated in PB combustion particles compared to MH PM. However, some trace elements such as lead, copper and calcium also showed higher concentrations of MH- than in PB-combustion PM.

Higher molecular weight polycyclic aromatic hydrocarbons (PAH, 4-ring and larger) and oxygenated PAH have been analyzed as they are toxicologically well-established organic PM compounds. The sum values of these compounds are depicted in Fig. 2E, showing that they were by an order of magnitude more abundant in the MH combustion particles compared to PB. This has been found for almost all PAH and PAH-derivatives with the exception of coronene (Fig. S5B).

The carboxylic compounds, another important class of air toxicants, were also found to be an order of magnitude more enriched in MH combustion aerosols compared to the PB combustion aerosols (see Fig. S6A). Other organic gas phase compounds, such as smaller polycyclic aromatic compounds (2- and 3-ring PAH) and benzene derivatives were more concentrated in MH combustion aerosols compared to the PB combustion aerosols as well (Fig. S6B).

Of particular interest regarding biological effects are semi-volatile phenolic compounds (Fig. 3A) or polyphenolic compounds [56]. The concentration of phenolic species in the PM from PB emissions was between 1 and 3 orders of magnitude lower when compared with log wood emissions. The quality of combustion in terms of completeness, which is influenced by the combustion technology and temperature as well as the size and type of fuel, is inversely correlated with the number and length of substituents on aromatic rings [57]. The PB exhibited a more effective combustion and therefore generated emission with lower organic content and phenolic compounds. In general, the phenolic compounds in wood combustion originate from pyrolysis of the wood's structural polyphenolic polymer lignin. Similarly, the formation of larger polyphenolic species (oxidized aromatic structures) stems from the lignin-degradation with less breakdown of the lignin structure [58–60].

To gain a more profound insight, the oxidized aromatic structures in the MH and PB combustion particulate matter were also analyzed by electrospray ionization fourier transform ion cyclotron resonance mass spectrometry (ESI- FTICR MS) at the molecular level. For the
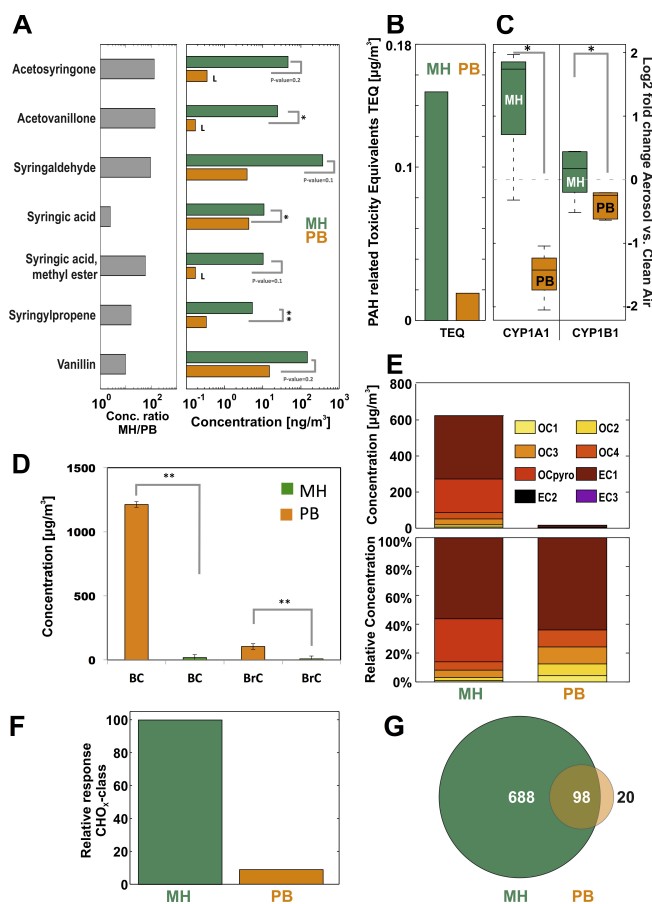
Fig. 3. Chemical characterization results of antioxidant content and PAHs in exposure aerosols. (A) Phenols were more abundant in MH emission aerosols in comparison to the PB emissions. (B) PAH-related toxicity equivalent values (TEQ) were calculated based on the proposal of the German Research Foundation (DFG) [55]. (C) The genes CYP1A1 and CYP1B1 were activated after exposure of A549 cells to the MH combustion aerosol, consistent with high TEQ values. (D) Black Carbon (BC, ∼ soot) and brown carbon (BrC, ∼ light absorbing organics) were very abundant in the MH combustion particles. (E) Representation of the thermo-optical carbon analysis (TOCA). (F) Venn plot depicted from ultra-high mass resolution analyses (FTICR) of the water-soluble PM components shows that the total amount of detectable organic compounds is by a factor of about 7 higher for beech log wood than for pellet particles. (G) The signal intensity of oxygen-containing compounds (CHO class) is more than an order of magnitude higher for the log wood group. L = limit of quantification, * = *p*-value < 0.05, ** = *p*-value < 0.005.

MH sample, negative polarity ESI spectra contained 760 different oxygen-containing aromatic signals (i.e. molecular formulas) on average. In contrast, the PB samples showed a much lower number of signals (118) with lower total intensity (integrated signal strength for oxygen-containing aromatic signals for PB PM was ∼ 1/16 of the one for MH PM). Highly aromatic and highly oxidized species were found in the water-soluble organic carbon fraction of the MH combustion particulate matter, whereas being nearly absent for the PB combustion (for ESI with negative and positive ion polarity). A high amount of species with a double bond equivalent larger than 4 and up to more than 12 with an average number of 2-5 oxygens was revealed. Intensity-weighted average values pointed to a higher aromaticity for the species detected in the MH combustion PM sample

compared to the PB (double bond equivalents of 8.68 ± 10% versus 7.40 ± 10%). The species found in the PB combustion experiments, albeit being of considerably lower intensity, covered a comparable chemical space to the MH combustion experiment. This suggests that chemical characteristics of the organic fraction in both cases are qualitatively comparable although much lower concentrations of oxygen-containing compound such as polyphenols were found in PB combustion PM due to the more complete combustion.

The Aethalometer measurements (Fig. 3D) revealed, that unlike PB combustion, the MH combustion formed PM containing violet/blue light (near UV) absorbing organic species (so-called brown carbon fraction, BrC). This is typical for formation of larger polyphenolic compounds from the lignin polymer [61–65] and is in line with the chemical ESI-FTICR MS analysis of the water-soluble oxidized PM species.

The thermal/optical carbon analysis TOCA (Fig. 3E) revealed that the contribution of the OC- as well as the EC-fractions, were negligible in the PB combustion PM. The MH combustion particles were dominated by the EC1- and OC pyro-fractions, indicating that heavier organic compounds were more important in this case. This could be attributed to the good combustion efficiency of the modern MH as simple log wood stoves can exhibit much higher OC1-OC3 contribution [66]. For MH log wood particles about 55% elemental carbon and 25% pyrolytically formed carbon were found, which was likely formed from charring of the wood polymers cellulose, hemicellulose and lignin in the measurement process. Very small amounts of carbon with dominating elemental carbon were consistently found with the optical analysis of the PB.

In summary, this study confirmed, that the more complete combustion in PB revealed considerably less air pollutant parameters. The PM- and most organic air toxicant-concentrations were markedly reduced compared to MH combustion [67]. In detail, the MH combustion aerosol showed a ∼ 3-fold higher particle mass concentration (PM2.5) and deposited dose, accompanied by a substantially larger exposure concentration of organic compounds such as aldehydes, PAH or oxidized PAH in comparison to PB combustion (Fig. 2E, F). Only inorganic compounds such as potassium and the cytotoxic zinc were more abundant in PB emissions, indicating higher burning bed temperatures in the PB (Fig. 2D).

3.2. Biological effects of MH and PB emission aerosols in ALI exposed A549 cells

We now wished to compare the results from the chemical and physical characterization of wood combustion aerosols to biological effects on cultured human cells. To this end, human NSCLC A549 cells were exposed to the MH and PB emissions using an ALI-exposure system. Cellular membrane integrity assays via LDH release to the exogenous medium after each exposure proved the lack of cytotoxicity in all 4 h exposure experiments (Fig. S7B). The molecular response of these human lung cells was investigated in detail using transcriptomics and proteomics analyses.

The integral biological impact in A549 cells, measured by the overall changes in proteome and transcriptome was relatively mild after MH and PB combustion aerosol exposure (Fig. 4). According to the literature the PB combustion was less toxic than MH via a vis several endpoints [15].

The gene ontology based analysis of the A549 cells on the transcriptomic level in response to MH log combustion aerosols revealed
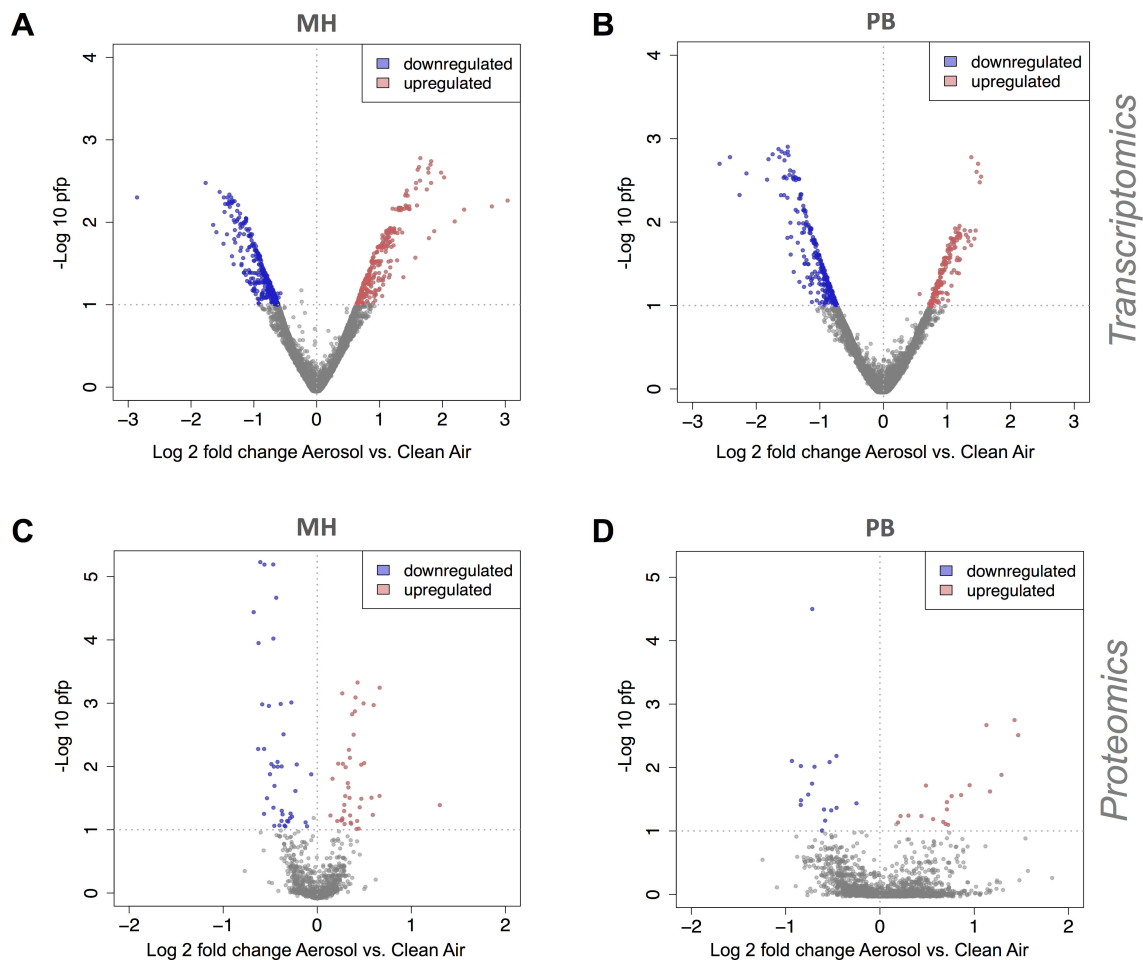
Fig. 4. Rank-product based regulation of proteins and mRNAs in ALI exposed A549 cells. Rank-product [40] was used to detect differentially expressed genes and proteins between aerosol and clean air treatment groups for transcriptomics data in response to (A) MH and (B) PB and for proteomics data in response to (C) MH and (D) PB combustion aerosols. The 2.5% most upregulated and downregulated genes with pfp < 0.1 and 25% most upregulated and downregulated proteins with pfp < 0.1 were considered as differentially regulated and selected for further analysis.

induction of signaling pathway like JAK-STAT and MAPK and a pro-inflammatory response. The exposure of A549 cells to the PB combustion aerosols mainly influenced cellular transport processes (Fig. 5). The gene-ontology based proteomics analysis revealed the induction of some DNA damage associated proteins in response to both, PB (MGMT and TIGAR) and MH (SMARCAD1, UBE2V2, and KAT5) emissions (Fig. 6), whereas no DNA damage was induced at the transcriptomic level (Fig. 5). It is known from the literature that, TIGAR for example, regulates DNA damage and repair and SMARCAD1 is involved DNA double-strand DNA break repair [68, 69]. This finding can be explained by assuming an immediate response of the proteome e.g. by stabilizing the already synthesized proteins, while the transcriptome shows the shut-down of the system in a time-delayed response.

Further conclusions can be drawn from a specific biological pathway analysis. The heat maps depicted in Fig. 7 show that several pro-inflammatory markers like IL8, IL24, IL6, and CCL20 for example, were induced after MH emission exposure and only IL6 was induced after the PB emission exposure. It was already shown under submersed conditions that exposure of A549 cells to the PM sample from MH increase in IL-8 production in a dose-dependent

way, while the PB combustion did not raise IL-8 levels above the background [15]. It has been shown in epidemiological studies that low-grade systemic inflammation might trigger the onset of cardiovascular and pulmonary diseases [70, 71]. Moreover, MAPK signaling was activated in response to the MH wood combustion aerosol. This could be due to the higher abundant carbon fraction, which was shown to activate MAPK in normal human bronchial epithelial cells [72]. After exposure of the A549 cells to the PB combustion aerosol, mostly intracellular transport processes were activated (Fig. 7).

Moreover, cytochrome P450 1A1 (CYP1A1) was induced by exposure to the MH combustion aerosol in A549 cells, in line with previous studies on wood smoke particles under submerged conditions [54]. Cyp1A1 is considered to be a key metabolic enzyme for the metabolism of benz[a]pyrene and related PAH structures corresponding to the highest benz[a]pyrene and PAH concentrations in MH combustion aerosol (Fig. S5B and 3C) [73]. The metabolism of PAHs requires metabolic activation by cytochrome P450 enzymes to more reactive metabolites [74, 75]. Since PAHs are hazardous due to their carcinogenic and mutagenic effects triggered by their genotoxic metabolites, its activation by the PAH-rich log wood emissions sug-
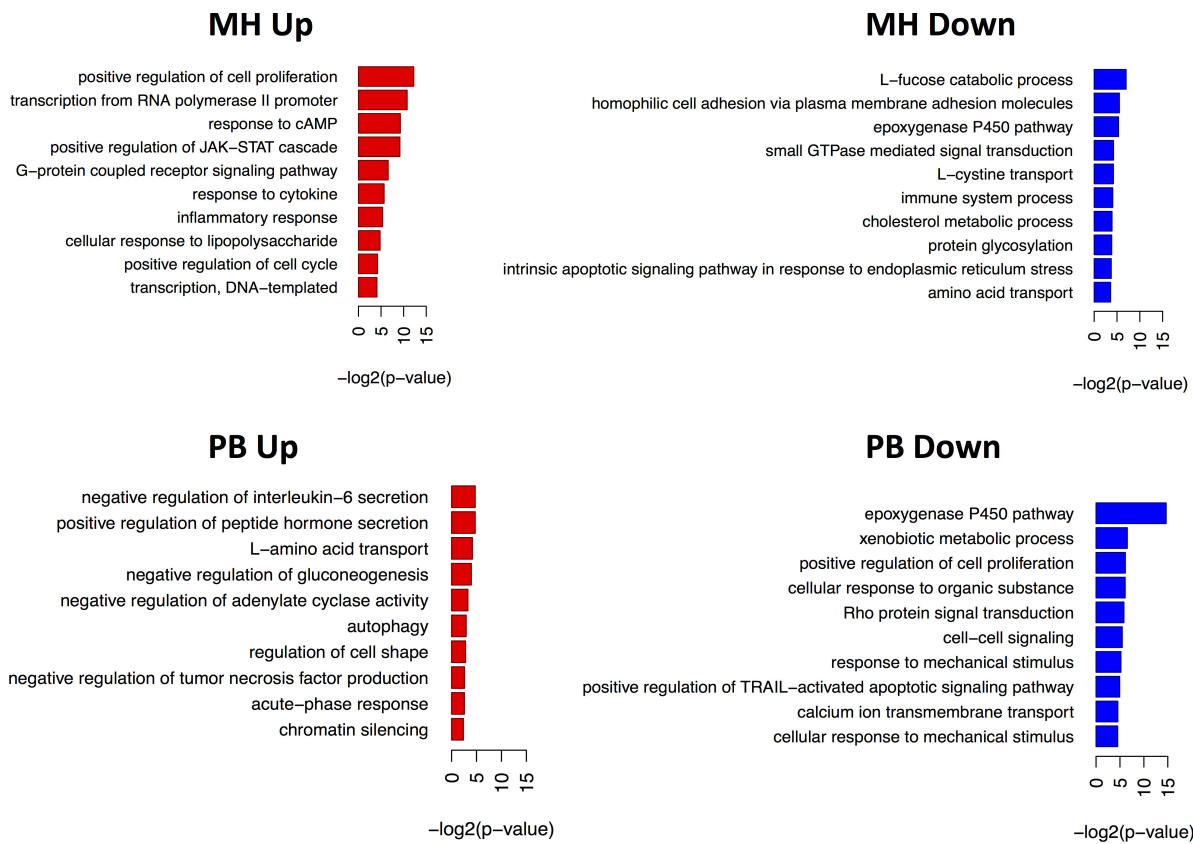
MH Up

positive regulation of cell proliferation
transcription from RNA polymerase II promoter
response to cAMP
positive regulation of JAK–STAT cascade
G–protein coupled receptor signaling pathway
response to cytokine
inflammatory response
cellular response to lipopolysaccharide
positive regulation of cell cycle
transcription, DNA–templated

−log2(p−value)

MH Down

L–fucose catabolic process
homophilic cell adhesion via plasma membrane adhesion molecules
epoxygenase P450 pathway
small GTPase mediated signal transduction
L–cystine transport
immune system process
cholesterol metabolic process
protein glycosylation
intrinsic apoptotic signaling pathway in response to endoplasmic reticulum stress
amino acid transport

−log2(p−value)

PB Up

negative regulation of interleukin–6 secretion
positive regulation of peptide hormone secretion
L–amino acid transport
negative regulation of gluconeogenesis
negative regulation of adenylate cyclase activity
autophagy
regulation of cell shape
negative regulation of tumor necrosis factor production
acute–phase response
chromatin silencing

−log2(p−value)

PB Down

epoxygenase P450 pathway
xenobiotic metabolic process
positive regulation of cell proliferation
cellular response to organic substance
Rho protein signal transduction
cell–cell signaling
response to mechanical stimulus
positive regulation of TRAIL–activated apoptotic signaling pathway
calcium ion transmembrane transport
cellular response to mechanical stimulus

−log2(p−value)

Fig. 5. Representation of induced biological pathways in ALI exposed A549 cells based on transcriptomics data. Regulated genes were used for the Gene Ontology analysis using the DAVID online tool [41].
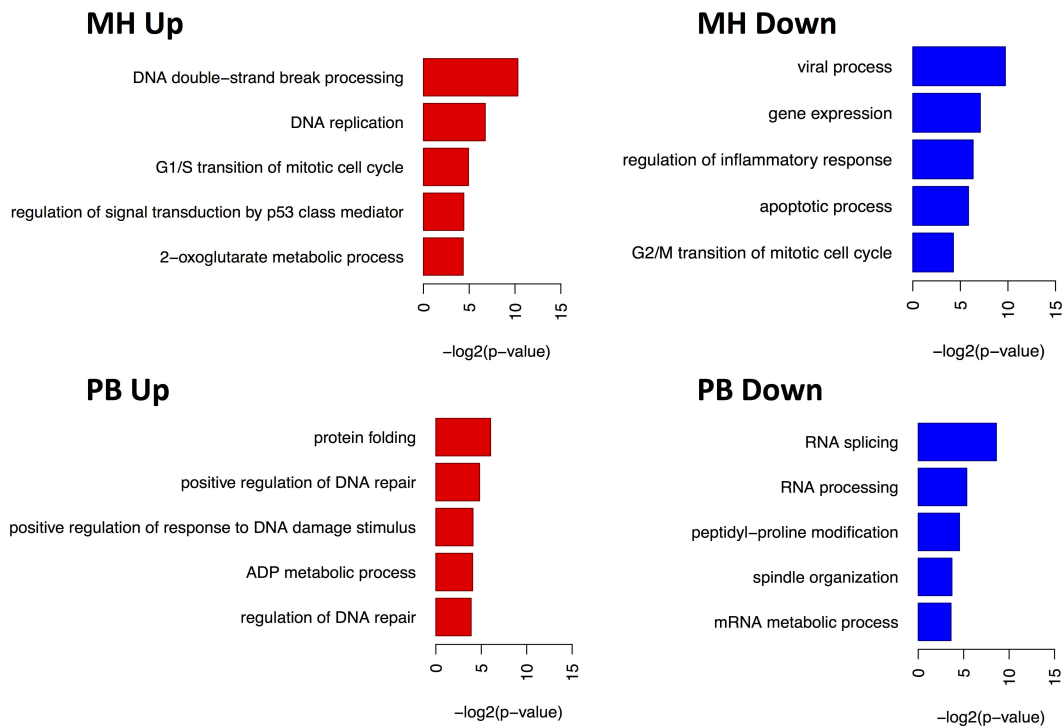
MH Up

DNA double–strand break processing
DNA replication
G1/S transition of mitotic cell cycle
regulation of signal transduction by p53 class mediator
2–oxoglutarate metabolic process

−log2(p−value)

MH Down

viral process
gene expression
regulation of inflammatory response
apoptotic process
G2/M transition of mitotic cell cycle

−log2(p−value)

PB Up

protein folding
positive regulation of DNA repair
positive regulation of response to DNA damage stimulus
ADP metabolic process
regulation of DNA repair

−log2(p−value)

PB Down

RNA splicing
RNA processing
peptidyl–proline modification
spindle organization
mRNA metabolic process

−log2(p−value)

Fig. 6. Representation of induced biological pathways in ALI exposed A549 cells based on proteomics data. Regulated proteins were used for the Gene Ontology analysis using the DAVID online tool [41].
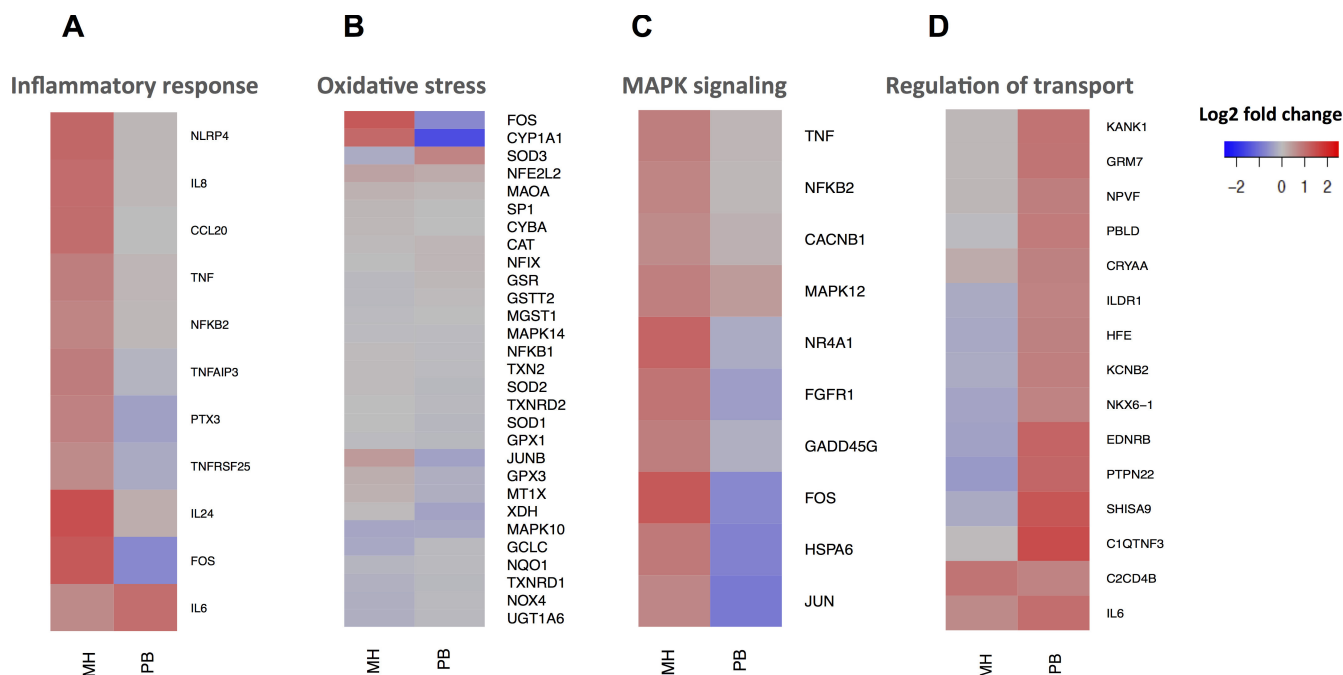
Fig. 7. Heat map representation of selected relevant genes in ALI exposed A549 cells based on transcriptomics data. Gene regulation of (A) inflammation, (B) oxidative stress, (C) MAPK signaling and (D) Regulation of transport.

gests that chronically adverse health effects might be more relevant in case of MH combustion compared to the PB emissions.

It was previously described that at high doses of wood smoke particles under submersed conditions, production of free radicals occurs, thereby inducing DNA damage as well as inflammatory and oxidative stress response gene expression in A549 cells [10]. However, in our present experiments, the applied dose of wood combustion aerosols was much lower in order to avoid enhanced cytotoxicity. Therefore, the acute sub-cytotoxic effect from MH combustion exposure was the induction of several pro-inflammatory markers and DNA double-strand break repair in the absence of significant induction of oxidative stress. Neither were oxidative stress associated genes induced after PB combustion aerosol exposure (Fig. 7B).

The comparison to the results from the shipping emissions study from Oeder et al., (2015) at similar to PB and 3-fold lower than MH deposition dose (Fig. S4A) showed that in contrast to the wood combustion aerosols DF particles strongly affected basic cellular functions such as energy metabolism, which indicated that mitochondrial stress was induced. Furthermore, mechanisms which are yet poorly known to be affected by aerosol treatment, such as RNA processing and chromatin modifications were activated, which reflected prominent proteomic and transcriptomic regulation (Fig. S7A) [28]. Most probably, the complete aerosol (the particles and the gases) from ship DF emission would cause even stronger effects. Phenolic compounds were more abundant in the wood combustion aerosols compared to shipping emissions and have been discussed as strongly antioxidative constituents of wood smoke in the literature (Fig. S4B) [56]. Moreover, the anti-oxidative compounds may be responsible for the previously observed lower relative toxicities of wood combustion aerosols in comparison with diesel car emissions (without particle filter) [56, 76–79]. Phenols and other oxygen-containing compounds are also potential trapping agents for electrophilic genotoxic com-

pounds that are considered to be carcinogenic [80]. It was already shown in the Boise campaign by Cupitt et al. (1994) that for the same dose of combustion material, the lifetime lung cancer risk was estimated to be much higher for the particles from mobile sources than for the particles from residential wood burning due to extractable organic matter [81]. Moreover, the high soot content in the MH particles could reduce the bioavailability of PM-associated air-toxicants by absorption of harmful substances on the carbon matrix (Fig. 2E). The soot in the carbonaceous fraction provides good adsorptive properties, thus many compounds can easily bind to it [82].

4. Summary

To identify possibly harmful cellular effects of wood combustion derived aerosols, extensive transcriptomics, and proteomics analyses was used in combination with chemical and physical aerosol characterization. This was targeted to assemble a broad overview of the cellular mechanisms affected by aerosol emissions of modern wood combustion compliances PB and MH. Our study revealed that the chemical compositions of the two wood combustion aerosols and their induced biological pathways differed largely. The PB, currently considered as very efficient renewable and clean way for residential heating, showed, in accordance with the literature, significantly lower emissions of PM and hazardous organic substances compared to the MH. The PB combustion was less toxic than MH in several endpoints, namely MAPK signaling, inflammatory response and CYP1A1 induction. Furthermore, diluted aerosol emissions of both compliances induced relatively mild biological responses, indicated by small changes in the proteome, in the exposed A549 cells when compared to equally diluted ship diesel engine emissions.

In conjunction with the preceding work on ship diesel emissions, the results of the current study suggest that it is difficult to estimate the (acute) toxicological impact of aerosol emissions just by the

PM$_{2.5}$ concentration or the concentration of specific chemical constituents and toxicants. This is caused by antagonistic and synergistic effects of different chemicals and aerosol properties.

Our findings support the previously described hypotheses that phenolic antioxidants, present in wood combustion aerosol, influence their toxicity and may mitigate adverse effects of some pollutants. This serves as a major motivation towards further studies to investigate the role of phenolic antioxidants, using aerosols with known properties and chemical composition from a combustion-aerosol generator, with defined spiking of phenolic compounds. In this study, primary emissions were investigated. As primary emissions will change quickly in the atmosphere, the aging of combustion aerosols will be included in further experiments.

Despite the relatively low subacute toxicity of the PB and MH emissions, the high concentration of genotoxic compounds suggests public health protection measures for application of residential wood heating in densely populated areas. In this context, filter systems for small-scale MHs as well as for PBs, which are either under development or are already available shall be promoted to reduce the health risks caused by residential wood combustion.

Acknowledgments

Conflict of Interest

The authors declare no conflict of interest.

Author Contributions

Conceived and designed the experiments: Tamara Kanashova, Olli Sippula, Sebastian Oeder, Thorsten Streibel, Johannes Passig, Hendryk Czech, Tony Kaoma, Sean C. Sapcariu, Marco Dilger, Hanns-Rudolf Paur, Christoph Schlager, Sonja Mülhopt, Carsten-Weiss, Carsten Schmidt-Weber, Claudia Traidl-Hoffmann, Bernhard Michalke, Tobias Krebs, Erwin Karg, Gert Jakobi, Sorana Scholtes, Jürgen Schnelle-Kreis, Martin Sklorz, Jürgen Orasche, Laarnie Müller, Ahmed Reda, Christopher Rüger, Anika Neumann, Gülcin Abbaszade, Christian Radischat, Karsten Hiller, Julija Grigonyte, Miika Kortelainen Kari Kuuspalo, Heikki Lamberg, Jani Leskinen, Ilpo Nuutinen, Tiina Torvela, Jarkko Tissari, Pasi Jalava, Stefanie Kasurinen, Oskari Uski, Maija-Riitta Hirvonen, Jeroen Buters, Gunnar Dittmar, Jorma K. Jokiniemi and Ralf Zimmermann.

Performed the experiments: Tamara Kanashova, Olli Sippula, Sebastian Oeder, Hendryk Czech, Sean C. Sapcariu, Marco Dilger, Christoph Schlager, Gert Jakobi, Jürgen Orasche, Laarnie Müller, Ahmed Reda, Christopher Rüger, Anika Neumann, Gülcin Abbaszade, Christian Radischat, Miika Kortelainen, Kari Kuuspalo, Heikki Lamberg, Jani Leskinen, Ilpo Nuutinen, Tiina Torvela, Jarkko Tissari, Pasi Jalava, Stefanie Kasurinen, Oskari Uski.

Performed physical and chemical characterization: Olli Sippula, Thorsten Streibel, Hendryk Czech, Gert Jakobi, Jürgen Orasche, Laarnie Müller, Ahmed Reda, Christopher Rüger, Anika Neumann, Erwin Karg, Gülcin Abbaszade, Christian Radischat, Martin Sklorz, Jürgen Schnelle-Kreis.

Performed proteomic analysis: Tamara Kanashova.

Performed transcriptome analysis: Sebastian Oeder.

Performed bioinformatic analysis: Tamara Kanashova, Tony Kaoma, Gunnar Dittmar, Sebastian Oeder.

Wrote the paper: Tamara Kanashova, Johannes Passig.

Initially conceived and designed the study: Ralf Zimmermann.

References

[1] Brunekreef B, Holgate ST. Air pollution and health. *Lancet*, 2002; 360(9341): 1233–1242.

[2] World Health Organization, Systematic review of air pollution, a global update. *Geneva, World Health Organization*, 2006.

[3] Pope III CA, Dockery DW. Health effects of fine particulate air pollution: lines that connect. *Journal of the Air & Waste Management Association*, 2006; 56(6): 709–742.

[4] Lepeule J, Laden F, Dockery D, Schwartz J. Chronic exposure to fine particles and mortality: an extended follow-up of the Harvard Six Cities study from 1974 to 2009. *Environ Health Persp*, 2012; 120(7): 965.

[5] Cesaroni G, Forastiere F, Stafoggia M, Andersen ZJ, Badaloni C, Beelen R, *et al.* Long term exposure to ambient air pollution and incidence of acute coronary events: prospective cohort study and meta-analysis in 11 European cohorts from the ESCAPE Project. *Bmj*, 2014; 348: f7412.

[6] Cohen AJ, Brauer M, Burnett R, Anderson HR, Frostad J, Estep K, *et al.* Estimates and 25-year trends of the global burden of disease attributable to ambient air pollution: an analysis of data from the Global Burden of Diseases Study 2015. *Lancet*, 2017; 389(10082): 1907–1918.

[7] Karagulian F, Belis CA, Dora CFC, Prüss-Ustün AM, Bonjour S, Adair-Rohani H, *et al.* Contributions to cities' ambient particulate matter (PM): A systematic review of local source contributions at global level. *Atmos Environ*, 2015; 120: 475–483.

[8] Salvi S, Barnes PJ. Is exposure to biomass smoke the biggest risk factor for COPD globally? *Chest*, 2010; 138(1): 3–6.

[9] Olloquequi J, Silva O R. Biomass smoke as a risk factor for chronic obstructive pulmonary disease: effects on innate immunity. *Innate Immun-London*, 2016; 22(5): 373–381.

[10] Danielsen PH, Møller P, Jensen KA, Sharma AK, Wallin H, Bossi R, *et al.* Oxidative stress, DNA damage, and inflammation induced by ambient air and wood smoke particulate matter in human A549 and THP-1 cell lines. *Chem Res Toxicol*, 2011; 24 (2): 168–184.

[11] Corsini E, Budello S, Marabini L, Galbiati V, Piazzalunga A, Barbieri P, *et al.* Comparison of wood smoke PM2. 5 obtained from the combustion of FIR and beech pellets on inflammation and DNA damage in A549 and THP-1 human cell lines. *Arch Toxicol*, 2013; 87(12): 2187–2199.

[12] Bølling AK, Pagels J, Yttri KE, Barregard L, Sallsten G, Schwarze PE, *et al.* Health effects of residential wood smoke particles: the importance of combustion conditions and physicochemical particle properties. *Part Fibre Toxicol*, 2009; 6(1): 29.

[13] Jalava PI, Happo MS, Kelz J, Brunner T, Hakulinen P, Mäki-Paakkanen J, *et al.* In vitro toxicological characterization of particulate emissions from residential biomass heating systems based on old and new technologies. *Atmos Environ*, 2012; 50: 24–35.

[14] Uski O, Jalava P, Happo M, Torvela T, Leskinen J, Mäki-Paakkanen J, *et al.* Effect of fuel zinc content on toxicological responses of particulate matter from pellet combustion in vitro. *Sci Total Environ*, 2015; 511: 331–340.

[15] Kasurinen S, Jalava PI, Happo MS, Sippula O, Uski O, Koponen H, *et al.* Particulate emissions from the combustion of birch, beech, and spruce logs cause different cytotoxic responses in A549 cells. *Environ Toxicol*, 2017; 32(5): 1487–1499.

[16] Naeher LP, Brauer M, Lipsett M, Zelikoff JT, Simpson CD, Koenig JQ, *et al.* Woodsmoke health effects: a review. *Inhal Toxicol*, 2007; 19(1): 67–106.

[17] Association EB, *et al.* AEBIOM Statistical Report 2015. 2015.

[18] Boman C, Pettersson E, Westerholm R, Bostro?m D, Nordin A. Stove performance and emission characteristics in residential wood log and pellet combustion, part 1: pellet stoves. *Energ Fuel*, 2011; 25(1): 307–314.

[19] Orasche J, Schnelle-Kreis J, Abbaszade G, Zimmermann R. In-situ derivatization thermal desorption GC-TOFMS for direct analysis of particle-bound non-polar and polar organic species. *Atmos Chem Phys*, 2011; 11(17): 8977–8993.

[20] Ozgen S, Caserini S, Galante S, Giugliano M, Angelino E, Marongiu A, *et al.* Emission factors from small scale appliances burning wood and pellets. *Atmos Environ*, 2014; 94: 144–153.

[21] Reda AA, Czech H, Schnelle-Kreis J, Sippula O, Orasche J, Weggler B, *et al.* Analysis of gas-phase carbonyl compounds in emissions from modern wood combustion appliances: influence of wood type and combustion appliance. *Energ Fuel*, 2015; 29 (6): 3897–3907.

[22] Sehlstedt M, Dove R, Boman C, Pagels J, Swietlicki E, Löndahl J, *et al.* Antioxidant airway responses following experimental exposure to wood smoke in man. *Part Fibre Toxicol*, 2010; 7 (1): 21.

[23] Holder AL, Lucas D, Goth-Goldstein R, Koshland CP. Cellular response to diesel exhaust particles strongly depends on the exposure method. *Toxicol Sci*, 2008; 103(1): 108–115.

[24] Aufderheide M, Mohr U. CULTEX—an alternative technique for cultivation and exposure of cells of the respiratory tract to airborne pollutants at the air/liquid interface. *Exp Toxicol Pathol*, 2000; 52(3): 265–270.

[25] Gasser M, Riediker M, Mueller L, Perrenoud A, Blank F, Gehr P, *et al.* Toxic effects of brake wear particles on epithelial lung cells in vitro. *Part Fibre Toxicol*, 2009; 6(1): 30.

[26] Mülhopt S, Dilger M, Diabaté S, Schlager C, Krebs T, Zimmermann R, *et al.* Toxicity testing of combustion aerosols at the air–liquid interface with a self-contained and easy-to-use exposure system. *J Aerosol Sci*, 2016; 96: 38–55.

[27] Paur HR, Cassee FR, Teeguarden J, Fissan H, Diabate S, Aufderheide M, *et al.* In-vitro cell exposure studies for the assessment of nanoparticle toxicity in the lung—A dialog between aerosol science and biology. *J Aerosol Sci*, 2011; 42(10): 668–692.

[28] Oeder S, Kanashova T, Sippula O, Sapcariu SC, Streibel T, Arteaga-Salas JM, *et al.* Particulate matter from both heavy fuel oil and diesel fuel shipping emissions show strong biological effects on human lung cells at realistic and comparable in vitro exposure conditions. *PloS One*, 2015; 10(6): e0126536.

[29] Sapcariu SC, Kanashova T, Dilger M, Diabaté S, Oeder S, Passig J, *et al.* Metabolic profiling as well as stable isotope assisted metabolic and proteomic analysis of RAW 264.7 macrophages exposed to ship engine aerosol emissions: different effects of heavy fuel oil and refined diesel fuel. *PloS One*, 2016; 11(6): e0157964.

[30] Nuutinen K, Jokiniemi J, Sippula O, Lamberg H, Sutinen J, Horttanainen P, *et al.* Effect of air staging on fine particle, dust and gaseous emissions from masonry heaters. *Biomass Bioenerg*, 2014; 67: 167–178.

[31] Lamberg H, Nuutinen K, Tissari J, Ruusunen J, Yli-Pirilä P, Sippula O, *et al.* Physicochemical characterization of fine particles from small-scale wood combustion. *Atmos Environ*, 2011; 45 (40): 7635–7643.

[32] Ong SE, Mann M. A practical recipe for stable isotope labeling by amino acids in cell culture (SILAC). *Nat Protoc*, 2006; 1(6): 2650–2660.

[33] Mülhopt S, Diabaté S, Krebs T, Weiss C, Paur H. Lung toxicity determination by in vitro exposure at the air liquid interface with an integrated online dose measurement. in *Journal of Physics: Conference Series*, Vol. 170, number 1. 2009. IOP Publishing.

[34] Sapcariu SC, Kanashova T, Weindl D, Ghelfi J, Dittmar G, Hiller K. Simultaneous extraction of proteins and metabolites from cells in culture. *MethodsX*, 2014; 1: 74–80.

[35] Kanashova T, Popp O, Orasche J, Karg E, Harndorf H, Stengel B, *et al.* Differential proteomic analysis of mouse macrophages exposed to adsorbate-loaded heavy fuel oil derived combustion particles using an automated sample-preparation workflow. *Anal Bioanal Chem*, 2015; 407(20): 5965–5976.

[36] Rappsilber J, Ishihama Y, Mann M. Stop and go extraction tips for matrix-assisted laser desorption/ionization, nanoelectrospray, and LC/MS sample pretreatment in proteomics. *Anal Chem*, 2003; 75(3): 663–670.

[37] Cox J, Mann M. MaxQuant enables high peptide identification rates, individualized ppb-range mass accuracies and proteome-wide protein quantification. *Nat Biotechnol*, 2008; 26(12): 1367–1372.

[38] R Core Team. R: A language and environment for statistical computing. R Foundation for Statistical Computing, Vienna, Austria. URL: *http://www.R-project.org/*. 2014.

[39] Johnson WE, Li C, Rabinovic A. Adjusting batch effects in microarray expression data using empirical Bayes methods. *Biostatistics*, 2007; 8(1): 118–127.

[40] Breitling R, Armengaud P, Amtmann A, Herzyk P. Rank products: a simple, yet powerful, new method to detect differentially regulated genes in replicated microarray experiments. *FEBS Lett*, 2004; 573(1-3): 83–92.

[41] Huang DW, Sherman BT, Lempicki RA. Systematic and integrative analysis of large gene lists using DAVID bioinformatics resources. *Nat Protoc*, 2008; 4(1): 44.

[42] Shafizadeh F. Introduction to pyrolysis of biomass. *J Anal Appl Pyrol*, 1982; 3(4): 283–305.

[43] United States Environmental Protection Agency (USEPA). Integrated Risk Information System (IRIS); National Center for Environmental Assessment: Washington, DC (*http://www.epa.gov/iris*).

[44] Wiedensohlet A, Orsini D, Covert D, Coffmann D, Cantrell W, Havlicek M, *et al.* Intercomparison study of the size-dependent counting efficiency of 26 condensation particle counters. *Aerosol Sci Tech*, 1997; 27(2): 224–242.

[45] Bitterle E, Karg E, Schroeppel A, Kreyling W, Tippe A, Ferron G, *et al.* Dose-controlled exposure of A549 epithelial cells at the air–liquid interface to airborne ultrafine carbonaceous particles. *Chemosphere*, 2006; 65(10): 1784–1790.

[46] Paur HR, Mülhopt S, Weiss C, Diabaté S. In vitro exposure systems and bioassays for the assessment of toxicity of nanoparticles to the human lung. *Journal für Verbraucherschutz und Lebensmittelsicherheit*, 2008; 3(3): 319–329.

[47] Comouth A, Saathoff H, Naumann KH, Muelhopt S, Paur HR, Leisner T. Modelling and measurement of particle deposition for cell exposure at the air–liquid interface. *J Aerosol Sci*, 2013; 63: 103–114.

[48] Arnott WP, Hamasha K, Moosmüller H, Sheridan PJ, Ogren JA. Towards aerosol light-absorption measurements with a 7-wavelength aethalometer: Evaluation with a photoacoustic instrument and 3-wavelength nephelometer. *Aerosol Sci Tech*, 2005; 39(1): 17–29.

[49] Elsasser M, Busch C, Orasche J, Scho?n C, Hartmann H, Schnelle-Kreis J, *et al.* Dynamic changes of the aerosol composition and concentration during different burning phases of wood combustion. *Energ Fuel*, 2013; 27(8): 4959–4968.

[50] Czech H, Sippula O, Kortelainen M, Tissari J, Radischat C, Passig J, *et al.* On-line analysis of organic emissions from residential wood combustion with single-photon ionisation time-of-flight mass spectrometry (SPI-TOFMS). *Fuel*, 2016; 177: 334–342.

[51] Tippe A, Heinzmann U, Roth C. Deposition of fine and ultrafine aerosol particles during exposure at the air/cell interface. *J Aerosol Sci*, 2002; 33(2): 207–218.

[52] Echalar F, Gaudichet A, Cachier H, Artaxo P. Aerosol emissions by tropical forest and savanna biomass burning: characteristic trace elements and fluxes. *Geophys Res Lett*, 1995; 22(22): 3039–3042.

[53] Schnelle-Kreis J, Sklorz M, Orasche J, Stölzel M, Peters A, Zimmermann R. Semi volatile organic compounds in ambient PM2. 5. Seasonal trends and daily resolved source contributions. *Environ Sci Technol*, 2007; 41(11): 3821–3828.

[54] Dilger M, Orasche J, Zimmermann R, Paur HR, Diabaté S, Weiss C. Toxicity of wood smoke particles in human A549 lung epithelial cells: the role of PAHs, soot and zinc. *Arch Toxicol*, 2016; 90(12): 3029–3044.

[55] Greim H. Gesundheitsschädliche Arbeitsstoffe; Toxikologisch-arbeitsmedizinische Begründungen von MAK-Werten und Einstufungen.(534) Weinheim, DFG, Deutsche Forschungsgemeinschaft. 2008: *Wiley-VCH Verlag.*

[56] Kjällstrand J, Petersson G. Phenolic antioxidants in wood smoke. *Sci Total Environ*, 2001; 277(1): 69–75.

[57] Czech H, Miersch T, Orasche J, Abbazade G, Sippula O, Tissari J, *et al.* Chemical composition and speciation of particulate organic matter from modern residential small-scale wood combustion appliances. *Sci Total Environ*, 2018; 612: 636–648.

[58] Simoneit BR, Rogge W, Mazurek M, Standley L, Hildemann L, Cass G. Lignin pyrolysis products, lignans, and resin acids as specific tracers of plant classes in emissions from biomass combustion. *Environ Sci Technol*, 1993; 27(12): 2533–2541.

[59] Rogge WF, Hildemann LM, Mazurek MA, Cass GR, Simoneit BR. Sources of fine organic aerosol. 9. Pine, oak, and synthetic log combustion in residential fireplaces. *Environ Sci Technol*, 1998; 32(1): 13–22.

[60] Nolte CG, Schauer JJ, Cass GR, Simoneit BR. Highly polar organic compounds present in wood smoke and in the ambient atmosphere. *Environ Sci Technol*, 2001; 35(10): 1912–1919.

[61] Wornat MJ, Ledesma EB, Marsh ND. Polycyclic aromatic hydrocarbons from the pyrolysis of catechol (ortho-dihydroxybenzene), a model fuel representative of entities in tobacco, coal, and lignin. *Fuel*, 2001; 80(12): 1711–1726.

[62] Ledesma EB, Marsh ND, Sandrowitz AK, Wornat MJ. Global kinetic rate parameters for the formation of polycyclic aromatic hydrocarbons from the pyrolyis of catechol, a model compound representative of solid fuel moieties. *Energ Fuel*, 2002; 16(6): 1331–1336.

[63] Marsh ND, Ledesma EB, Sandrowitz AK, Wornat MJ. Yields of Polycyclic Aromatic Hydrocarbons from the Pyrolysis of Catechol [o rtho-Dihydroxybenzene]: Temperature and Residence Time Effects. *Energ Fuel*, 2004; 18(1): 209–217.

[64] Fitzpatrick E, Ross A, Bates J, Andrews G, Jones J, Phylaktou H, *et al.* Emission of oxygenated species from the combustion of pine wood and its relation to soot formation. *Process Saf Environ*, 2007; 85(5): 430–440.

[65] Fitzpatrick E, Jones J, Pourkashanian M, Ross A, Williams A, Bartle K. Mechanistic aspects of soot formation from the combustion of pine wood. *Energ Fuel*, 2008; 22(6): 3771–3778.

[66] Diab J, Streibel T, Cavalli F, Lee S, Saathoff H, Mamakos A, *et al.* Hyphenation of a EC/OC thermal–optical carbon analyzer to photo-ionization time-of-flight mass spectrometry: an off-line aerosol mass spectrometric approach for characterization of primary and secondary particulate matter. *Atmos Meas Tech*, 2015; 8(8): 3337.

[67] Orasche J, Seidel T, Hartmann H, Schnelle-Kreis J, Chow JC, Ruppert H, *et al.* Comparison of emissions from wood combustion. Part 1: Emission factors and characteristics from different small-scale residential heating appliances considering particulate matter and polycyclic aromatic hydrocarbon (PAH)-related toxicological potential of particle-bound organic species. *Energ Fuel*, 2012; 26(11): 6695–6704.

[68] Yu HP, Xie JM, Li B, Sun YH, Gao QG, Ding ZH, *et al.* TIGAR regulates DNA damage and repair through pentosephosphate pathway and Cdk5-ATM pathway. *Sci Rep-Uk*, 2015; 5: 9853.

[69] Bantele SC, Ferreira P, Gritenaite D, Boos D, Pfander B. Targeting of the Fun30 nucleosome remodeller by the Dpb11 scaffold facilitates cell cycle-regulated DNA end resection. *eLife*, 2017; 6: e21687.

[70] Kim KH, Kabir E, Kabir S. A review on the human health impact of airborne particulate matter. *Environ Int*, 2015; 74: 136–143.

[71] Berend N. Contribution of air pollution to COPD and small airway dysfunction. *Respirology*, 2016; 21(2): 237–244.

[72] Kim YM, Reed W, Lenz AG, Jaspers I, Silbajoris R, Nick HS, *et al.* Ultrafine carbon particles induce interleukin-8 gene transcription and p38 MAPK activation in normal human bronchial epithelial cells. *Am J Physiol-Lung C*, 2005; 288(3): L432–L441.

[73] Shimada T, Fujii-Kuriyama Y. Metabolic activation of polycyclic aromatic hydrocarbons to carcinogens by cytochromes P450 1A1 and1B1. *Cancer Sci*, 2004; 95(1): 1–6.

[74] Conney AH. Induction of microsomal enzymes by foreign chemicals and carcinogenesis by polycyclic aromatic hydrocarbons: GHA Clowes Memorial Lecture. *Cancer Res*, 1982; 42 (12): 4875–4917.

[75] Guengerich FP, Shimada T. Oxidation of toxic and carcinogenic chemicals by human cytochrome P-450 enzymes. *Chem Res Toxicol*, 1991; 4(4): 391–407.

[76] Kubátová A, Steckler TS, Gallagher JR, Hawthorne SB, Picklo MJ. Toxicity of wide-range polarity fractions from wood smoke and diesel exhaust particulate obtained using hot pressurized water. *Environ Toxicol Chem*, 2004; 23(9): 2243–2250.

[77] Kubátová A, Dronen LC, Picklo MJ, Hawthorne SB. Midpolarity and nonpolar wood smoke particulate matter fractions deplete glutathione in RAW 264.7 macrophages. *Chem Res Toxicol*, 2006; 19(2): 255–261.

[78] Bølling AK, Pagels J, Yttri KE, Barregard L, Sallsten G, Schwarze PE, *et al.* Health effects of residential wood smoke particles: the importance of combustion conditions and physicochemical particle properties. *Part Fibre Toxicol*, 2009; 6(1): 29.

[79] Nićiforović N, Abramovič H. Sinapic acid and its derivatives: natural sources and bioactivity. *Compr Rev Food Sci*, 2014; 13 (1): 34–51.

[80] Newmark HL. Plant phenolics as potential cancer prevention agents. *Dietary Phytochemicals in Cancer Prevention and Treatment*, 1996; 25–34.

[81] Cupitt LT, Glen WG, Lewtas J. Exposure and risk from ambient particle-bound pollution in an airshed dominated by residential wood combustion and mobile sources. *Environ Health Persp*, 1994; 102(Suppl 4): 75.

[82] Gauggel-Lewandowski S, Heussner AH, Steinberg P, Pieterse B, van der Burg B, Dietrich DR. Bioavailability and potential carcinogenicity of polycyclic aromatic hydrocarbons from wood combustion particulate matter in vitro. *Chem-Biol Interact*, 2013; 206(2): 411–422.